Unsteady-State Pressure Distributions Created by a Well With a Single Infinite-Conductivity Vertical Fracture

ALAIN C. GRINGARTEN*
MEMBER SPE-AIME
HENRY J. RAMEY, JR.
R. RAGHAVAN**
MEMBERS SPE-AIME

U. OF CALIFORNIA AT BERKELEY
BERKELEY, CALIF.

STANFORD U.
STANFORD, CALIF.

INTRODUCTION

During the last few years, there has been an explosion of information in the field of well-test analysis. Because of increased physical understanding of transient fluid flow, it is possible to analyze the entire pressure history of a well test, not just long-time data as in conventional analysis.[1] It is now often possible to specify the time of beginning of the correct semilog straight line and determine whether the correct straight line has been properly identified. It is also possible to identify wellbore storage effects, and the nature of wellbore stimulation as to permeability improvement, or fracturing, and to quantitatively analyze those effects.

Such accomplishments have been augmented by attempts to understand the short-time pressure data from well testing — data that were often classified as too complex for analysis. One recent study of short-time pressure behavior[2] showed that it was important to specify the physical nature of the stimulation in considering the behavior of a stimulated well. That is, stating that the van Everdingen-Hurst infinitesimal skin effect was negative was not sufficient to define short-time well behavior. For instance, acidized (but not acid-fractured) and hydraulically fractured wells might not necessarily exhibit the same behavior at early times, even though they could possess the same value of negative skin effect.

In the same manner, hydraulic fracturing leading to horizontal or vertical fractures could produce the same skin effect, but with possibly different short-time pressure data. This could then provide a way to determine the orientation of fractures created by this type of well stimulation. In fact, it is generally agreed that hydraulic fracturing usually results in one vertical fracture, the plane of which includes the wellbore. Most studies of the flow behavior for a fractured well consider vertical fractures only.[3-11]

Yet it is also agreed that horizontal fractures *could* occur in shallow formations. Furthermore, it would appear that notch-fracturing would lead to horizontal fractures. Surprisingly, no detailed study of the horizontal fracture case had been performed until recently.[12] A solution to this problem was presented by Gringarten and Ramey.[13] In the course of their study, it was found that a large variety of new transient pressure behavior solutions useful in well and reservoir analysis could be constructed from instantaneous Green's functions.[14] Possibilities included a well with a single vertical fracture in an infinite reservoir, or at any location in a rectangle.

Although similar cases had been studied before by van Everdingen and Meyer,[11] and by Russell and Truitt,[8] there were confusing differences in their respective results, and small inconsistencies between the cases of Ref. 8 made short-time analysis impossible. Both explicit and implicit finite-difference solutions and finite-element solutions were made for the vertical fracture case of Russell and Truitt in an attempt to eliminate differences between Refs. 8 and 11, and internal differences between cases in Ref. 8. It was not possible to reach satisfactory conclusions for the short-time performance region with even very long computer runs with *either* finite-difference or finite-element[12] programs. For this reason, it was decided to evaluate analytical solutions to provide a sound basis for short-time analysis of field data. In the course of the work, to provide a direct comparison with the Russell and Truitt data it became necessary to develop analytical solutions for fracture cases in which the fluid entry flux along the fracture caused a constant pressure along the fracture (infinite fracture conductivity). It also appeared worthwhile to evaluate the new solutions so that vertical fracture behavior could be compared with horizontal fracture behavior in infinite reservoirs. The new solutions for vertically fractured wells are especially useful for short-time or type-curve analysis. Such an analysis can provide information concerning permeabilities, fracture

Original manuscript received in Society of Petroleum Engineers office June 12, 1972. Revised manuscript received Dec. 18, 1973. Paper (SPE 4051) was presented at the SPE-AIME 47th Annual Fall Meeting, held in San Antonio, Tex., Oct. 8-11, 1972.

*Now with French Geological Bureau, Orleans, France.
**Now with Amoco Production Co., Tulsa, Okla.

[1]References listed at end of paper.

length, and distance to a symmetrical drainage limit. Combination of short-time analysis with older conventional semilog analytical methods permits an extraordinary confidence level concerning the analysis of field data.

VERTICALLY FRACTURED WELL IN AN INFINITE RESERVOIR

We model a plane (zero-thickness) vertical fracture totally penetrating a horizontal, homogeneous, and isotropic reservoir initially at constant pressure. At time zero, a single-phase, slightly compressible fluid flows from the reservoir into the fracture at a constant total rate. The producing pressure is *uniform* over the fracture (infinite fracture conductivity). The pressure remains constant and equal to the initial pressure as distance from the well becomes infinitely large (infinite reservoir).

An analytical expression for the pressure distribution created by the plane vertical fracture may be obtained by the Green's function and product solution method,[22] using source functions presented by Gringarten and Ramey.[14] The condition of uniform pressure over the fracture at all times is satisfied, as indicated in Ref. 14, by dividing the half-fracture length x_f into M segments of length x_f/M, each with a uniform flux per unit area, q_m, (m = 1,M). The first segment extends from 0 to x_f/M, the second segment from x_f/M to $2x_f/M$, the mth segment from $[(m-1)x_f]/M$ to mx_f/M, and the last segment from $[(M-1)/M]x_f$ to x_f, as shown in Fig. 1. The q_m (m = 1,M) are determined by equating the pressure drops at the center of the segments, which provide $(M-1)$ equations, the mth equation being obtained from the condition of constant total production rate at all times:

$$\Delta p\left(\frac{2j-1}{2M}\,x_f,\ 0,\ t\right) = \Delta P\left(\frac{2j+1}{2M}\,x_f,\ 0,\ t\right) \qquad j=1,M-1 \quad \ldots(1)$$

$$2\sum_{m=1}^{M} q_m\left(\frac{x_f}{M}\right)h = q_f \qquad \ldots(2)$$

The pressure drop created by the fracture is obtained from Ref. 14, Table 5:

$$p_i - p_{x,y,t} = \frac{1}{\phi c}\int_0^t \left\{\sum_{m=1}^{M} q_m(\tau)\int_{\frac{(m-1)x_f}{M}}^{\frac{mx_f}{M}} \exp\left[-\frac{(x-x_w)^2+y^2}{4\eta(t-\tau)}\right]dx_w - \sum_{m=1}^{M} q_m(\tau)\int_{-\frac{mx_f}{M}}^{-\frac{(m-1)}{M}x_f} \exp\left[-\frac{(x-x_w)^2+y^2}{4\eta(t-\tau)}\right]dx_w\right\} \cdot \frac{d\tau}{4\pi\eta(t-\tau)} \qquad \ldots(3)$$

The coordinate system in Fig. 1 and Eq. 3 is different from that of Ref. 14, however. A similar scheme has been used by Muskat[15] for the steady-state pressure distribution created by a partially penetrating well, and has been suggested by Burns[16] for unsteady state. In the unsteady state, however, the method seems impractical: it was expected — and confirmed from a numerical simulation[21] — that the flux per unit area of fracture is not constant but varies in time. A system of M equations and M unknowns as represented by Eqs. 1 and 2 should thus be solved at each value of time.

Actually, this is not true practically, and the pressure distribution can be obtained by solving the system of equations only once. The flux distribution in the fracture at various times, as obtained from a numerical simulation, is shown in Fig. 2. It can be seen that the flux distribution is uniform at very early times, then it changes, and finally it reaches a steady state at some extended time, after which flow entering the fracture stabilizes. The pressure during the stabilized flow period is independent of the flux distribution history, and is the same as if the flux distribution had been equal to the final stabilized flux distribution at all times.

An analog to this interesting and useful fact

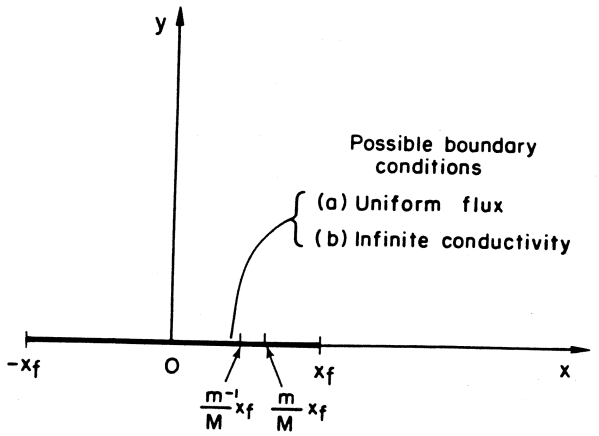

FIG. 1 — VERTICAL FRACTURE IN AN INFINITE RESERVOIR.

occurs in the case of flow to a constant-rate well with wellbore storage. Wellbore storage causes the sand-face production rate to change as a function of time initially. But after some initial period, the sand-face rate reaches the constant surface rate (within a specified percentage), and thereafter the producing pressure is equal to that of a well whose sand-face rate had been constant from the start of production. The pressure is independent of the production history! The same sort of observation was made in another reservoir problem by Carter and Tracy.[23]

By solving the system of Eqs. 1 and 2 for the *stabilized flux distribution* one can obtain a long-time solution for the pressure, whereas an early-time solution can be obtained by assuming uniform flux. We shall show that these also provide an excellent approximation for the pressure distribution at all times.

EARLY-TIME SOLUTION

Integrating Eq. 3 with respect to x_w, the dimensionless pressure drop can be written as

$$p_D(x_D,y_D,t_D) = \int_0^{t_D} \exp -\frac{y_D^2}{4(t-t')_D} \sum_{m=1}^{M} \left(\frac{2q_m(t_D')hx_f}{q_f}\right) \left[\operatorname{erf} \frac{x_D + \frac{m}{M}}{\sqrt{(t-t')_D}} - \operatorname{erf} \frac{x_D + \frac{m-1}{M}}{2\sqrt{(t-t')_D}} - \operatorname{erf} \frac{x_D - \frac{m}{M}}{2\sqrt{(t-t')_D}} + \operatorname{erf} \frac{x_D - \frac{m-1}{M}}{2\sqrt{(t-t')_D}}\right] \frac{dt_D'}{4[(t-t')_D/\pi]^{1/2}} \quad \ldots\ldots\ldots\ldots\ldots\ldots\ldots\ldots (4)$$

The dimensionless space and time variables in Eq. 4 are based on the fracture half-length x_f,

$$x_D = \frac{x}{x_f} \; ; \quad y_D = \frac{y}{x_f} , \quad \ldots\ldots\ldots (5)$$

and the dimensionless time and the dimensionless pressure drop are, respectively,

$$t_D = \frac{kt}{\phi\mu c x_f^2} , \quad \ldots\ldots\ldots\ldots\ldots (6)$$

and

$$p_D(x_D,y_D,t_D) = \frac{2\pi kh}{q_f\mu} (p_i - p_{x,y,t}) . \quad \ldots\ldots\ldots\ldots\ldots\ldots\ldots (7)$$

At very early times, the expression

$$\operatorname{erf} \frac{x_D \pm \frac{m}{M}}{2\sqrt{(t-t')_D}} - \operatorname{erf} \frac{x_D \pm \frac{m-1}{M}}{2\sqrt{(t-t')_D}}$$

becomes constant when t_D is small enough.[14] (The constant is 2 if $(m-1)/M < |x_D| < m/M$; unity if $|x_D| = (m-1)/M$ or $|x_D| = m/M$; and zero if $|x_D| < (m-1)/M$ or $|x_D| > m/M$.) Therefore, at very early times the system given by Eqs. 1 and 2 reduces to

$$\begin{cases} \displaystyle\int_0^{t_D} \exp\left[-\frac{y_D^2}{4(t-t')_D}\right] \frac{2q_j(t_D')hx_f}{q_f} \cdot \frac{dt_D'}{4[(t-t')_D/\pi]^{1/2}} = \int_0^{t_D} \exp\left[-\frac{y_D^2}{4(t-t')_D}\right] \cdot \frac{2q_{j+1}(t_D')hx_f}{q_f} \frac{dt_D'}{4[(t-t')_D/\pi]^{1/2}} , \\ \qquad - j=1, M-1 \quad \ldots\ldots\ldots (8) \\ \displaystyle\sum_{m=1}^{M} \frac{2q_m(t_D)hx_f}{q_f} = M , \quad \text{all } t_D , \\ \qquad \ldots\ldots\ldots (9) \end{cases}$$

which yields

$$q_j = \frac{q_f}{2hx_f} , \quad j=1,M .$$

As indicated by the numerical model, the flux must be uniform over the fracture at very early times, and the early-time solution for the pressure drop function is

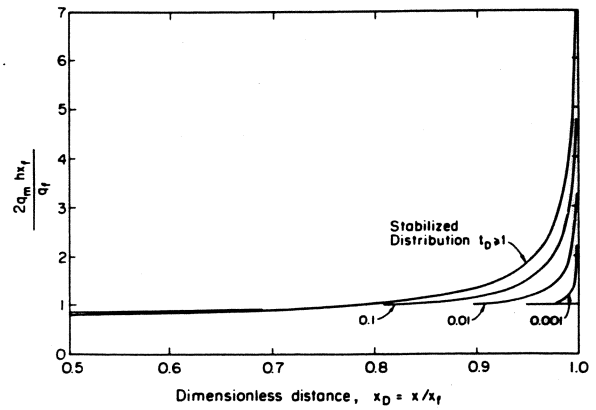

FIG. 2 — FLUX DISTRIBUTION AT VARIOUS TIMES ALONG AN INFINITE-CONDUCTIVITY VERTICAL FRACTURE (NUMERICAL MODEL).

$$p_D(|x_D|<1, y_D, t_D) =$$

$$\int_0^{t_D} \exp\left(-\frac{y_D^2}{4t'_D}\right) \frac{dt'_D}{2(t'_D/\pi)^{1/2}}$$

$$= (\pi t_D)^{\frac{1}{2}} \exp(-y_D^2/4t_D)$$

$$- |y_D| \operatorname{erfc}(|y_D|/2\sqrt{t_D}) \quad \ldots (10)$$

$$p_D(|x_D|>1, y_D, t_D) = 0$$

and, along the fracture,

$$p_{wD}(|x_D|<1, 0, t_D) = \sqrt{\pi t_D}, \quad \ldots (11)$$

which is the conventional result for flow in a linear system. In this case, there is flow into both sides of the fracture.

LONG-TIME SOLUTION

During the stabilized flow period, the q_m's are constant and can be taken out of the integral sign in Eq. 3. Inverting the order of integration in Eq. 3, one obtains

$$p_D(x_D, y_D, t_D) = \frac{1}{4} \sum_{m=1}^{M} \frac{2q_m h x_f}{q_f} \left\{ \int_{\frac{m-1}{M}}^{\frac{m}{M}} -Ei\left[-\frac{(x-x_w)_D^2 + y_D^2}{4t_D}\right] dx_{wD} \right.$$

$$\left. - \int_{-\frac{m}{M}}^{-\frac{m-1}{M}} - Ei\left[-\frac{(x-x_w)_D^2 + y_D^2}{4t_D}\right] \cdot dx_{wD} \right\}, \quad \ldots (12)$$

with

$$\sum_{m=1}^{M} \frac{2q_m h x_f}{q_f} = M \quad \ldots (13)$$

Substituting the series expansion of the exponential integral function into Eq. 12 yields the long-time solution for the dimensionless pressure drop function:

$$p_D(x_D, y_D, t_D) = \frac{1}{2}(\ln t_D + 2.80907) + \sigma(x_D, y_D), \quad \ldots (14)^*$$

where $\sigma(x_D, y_D)$ is a *pseudo skin function* that depends upon the position of the pressure point only:

$$\sigma(x_D, y_D) = \frac{1}{4} \sum_{m=1}^{M} \frac{2q_m h x_f}{q_f} \cdot \left\{ (x_D - \tfrac{m}{M}) \ln[y_D^2 + (x_D - \tfrac{m}{M})^2] \right.$$

$$- (x_D + \tfrac{m}{M}) \ln[y_D^2 + (x_D + \tfrac{m}{M})^2]$$

$$+ (x_D + \tfrac{m-1}{M}) \ln[y_D^2 + (x_D + \tfrac{m-1}{M})^2]$$

$$- (x_D - \tfrac{m-1}{M}) \ln[y_D^2 + (x_D - \tfrac{m-1}{M})^2]$$

$$- 2y_D \arctan\left[\frac{2y_D}{M}\left(r_D^2 + \frac{m(m-1)}{M^2}\right) \div \left([r_D^2 - (\tfrac{m}{M})^2][r_D^2 - (\tfrac{m-1}{M})^2] + \frac{4m(m-1)}{M^2} y_D^2\right)\right] \left.\right\} \quad \ldots (15)$$

where $r_D = r/x_f$ is the dimensionless distance to the axis of the fracture.

Eq. 14 has a form similar to the long-time approximation of the pressure function for radial flow[17] (i.e., a circular well without a fracture):

$$\frac{2\pi kh}{q\mu}(p_i - p_{r,t}) = \frac{1}{2}\left(\ln \frac{kt}{\phi \mu c r^2} + 0.80907\right), \quad r \geq r_w \quad \ldots (16)$$

As in the radial flow case, a straight line of slope 1.1515 per logarithmic cycle is obtained when the long-time dimensionless pressure drop is plotted vs the dimensionless flowing time on semilog coordinates. Thus, well test analysis methods developed for transient *radial* flow problems and based upon the existence of the 1.1515 slope semilog straight line, can be extended to analyze transient flow into a vertically fractured well in an infinite system. Actually, it can be shown that Eq. 14 becomes identical with Eq. 16 if x_f

*"2.80907" is correct.

tends to zero, of if r becomes very large.

The q_m's $(m-1,M)$ in Eq. 15 are obtained by solving the system of equations represented by Eqs. 1 and 2, which now reduces to

$$\left\{ \begin{array}{l} \sigma\left(\frac{2j-1}{2M},\ 0\right) = \sigma\left(\frac{2j+1}{2M},\ 0\right) \\ \qquad j = 1, M-1 \quad \ldots\ldots (17) \\ \sum_{m=1}^{M} \frac{2q_m h x_f}{q_f} = M \quad \ldots (18) \end{array} \right.$$

UNIFORM FLUX VERTICAL FRACTURE

This case corresponds to $M = 1$ and represents a first approximation of the behavior of a vertically fractured well. At early times, however, it is the exact solution.

The corresponding form of Eq. 4 is

$$p_D(x_D, y_D, t_D) = \int_0^{t_D} \exp\left(-\frac{y_D^2}{4t'_D}\right) \cdot \left[\operatorname{erf}\frac{1-x_D}{2\sqrt{t'_D}} + \operatorname{erf}\frac{1+x_D}{2\sqrt{t'_D}}\right] \frac{dt'_D}{4(t'_D/\pi)^{1/2}} \quad \ldots\ldots (19)$$

Eq. 19 cannot be expressed in terms of tabulated functions, and must be evaluated with a computer, except in the plane of the fracture ($y_D = 0$), where it becomes

$$p_D(x_D, 0, t_D) = \frac{1}{2}(\pi t_D)^{1/2}\left[\operatorname{erf}\frac{1-x_D}{2\sqrt{t_D}} + \operatorname{erf}\frac{1+x_D}{2\sqrt{t_D}}\right] - \frac{(1-x_D)}{4}\operatorname{Ei}\left[-\frac{(1-x_D)^2}{4t_D}\right] - \frac{(1+x_D)}{4}\operatorname{Ei}\left[-\frac{(1+x_D)^2}{4t_D}\right] \quad \ldots\ldots (20)$$

Eq. 20 shows that pressure will vary along the fracture length (except at early times), which would not be true if the fracture had infinite conductivity. However, the pressure drop along the fracture is low, and the uniform flux condition gives the appearance of a high, but not infinite, fracture conductivity. Some field data appear to match this solution better than the infinite-conductivity solution.

One useful expression for well test analysis is the pressure drop on the axis of the fracture ($x_D = 0$, $t_D = 0$):

$$p_{wD}(t_D) = \sqrt{\pi t_D}\ \operatorname{erf}\left(\frac{1}{2\sqrt{t_D}}\right) - \frac{1}{2}\operatorname{Ei}\left(-\frac{1}{4t_D}\right) \quad \ldots\ldots (21)$$

$p_{wD}(t_D)$ has been listed vs t_D in Table 1, and plotted in Figs. 3 and 4 as the $(x_e/x_f = \infty)$ curve.

Approximating forms of Eq. 19 at small and large values of time are the same as obtained in the previous section. The sigma pseudo skin function for the long-time approximation, Eq. 15, simplifies to

$$\sigma(x_D, y_D) = \frac{1}{4}\left\{(x_D-1)\ln[y_D^2 + (x_D-1)^2] - (x_D+1)\ln[y_D^2 + (x_D+1)^2] - 2y_D \arctan\frac{2y_D}{r_D^2 - 1}\right\} \quad \ldots (22)$$

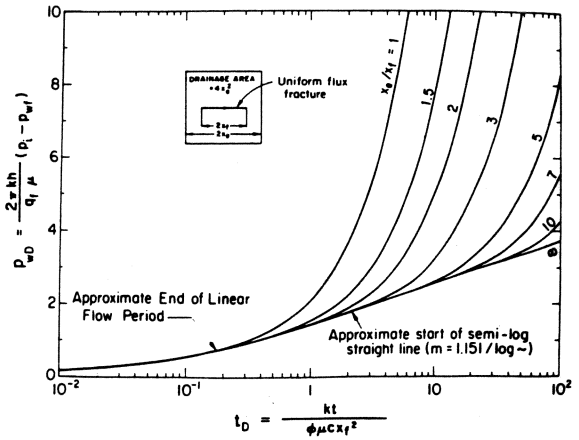

FIG. 3—p_{wD} VS t_D FOR A UNIFORM FLUX VERTICAL FRACTURE.

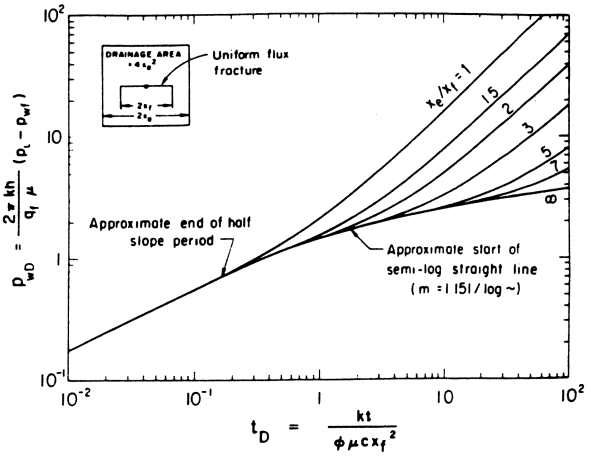

FIG. 4—p_{wD} VS t_D FOR A UNIFORM FLUX VERTICAL FRACTURE.

and in the plane of the fracture,

$$\sigma_D(x_D,0) = -\frac{1}{2}\left[(1-x_D)\ln|1-x_D| + (1+x_D)\ln|1+x_D|\right] \quad \ldots (23)$$

TABLE 1 — p_{wD} FOR A VERTICALLY FRACTURED WELL IN AN INFINITE RESERVOIR

t_D	Uniform flux	Infinite Conductivity
1.0E-02	0.1772	0.1765
1.5E-02	0.2171	0.2145
2.0E-02	0.2507	0.2456
3.0E-02	0.3070	0.2955
4.0E-02	0.3545	0.3356
5.0E-02	0.3963	0.3697
6.0E-02	0.4340	0.3996
8.0E-02	0.5007	0.4509
1.0E-01	0.5587	0.4945
1.5E-01	0.6790	0.5833
2.0E-01	0.7756	0.6549
3.0E-01	0.9261	0.7691
4.0E-01	1.0417	0.8603
5.0E-01	1.1355	0.9367
6.0E-01	1.2145	1.0027
8.0E-01	1.3427	1.1129
1.0E+00	1.4447	1.2030
1.5E+00	1.6344	1.3754
2.0E+00	1.7716	1.5032
3.0E+00	1.9676	1.6894
4.0E+00	2.1080	1.8248
5.0E+00	2.2175	1.9312
6.0E+00	2.3073	2.0189
8.0E+00	2.4494	2.1583
1.0E+01	2.5600	2.2673
1.5E+01	2.7613	2.4664
2.0E+01	2.9045	2.6085
3.0E+01	3.1065	2.8094
4.0E+01	3.2500	2.9524
5.0E+01	3.3614	3.0634
6.0E+01	3.4524	3.1542
8.0E+01	3.5961	3.2976
1.0E+02	3.7075	3.4089
1.5E+02	3.9101	3.6113
2.0E+02	4.0539	3.7549
3.0E+02	4.2566	3.9575
4.0E+02	4.4004	4.1012
5.0E+02	4.5119	4.2127
6.0E+02	4.6031	4.3039
8.0E+02	4.7469	4.4477
1.0E+03	4.8584	4.5592
1.5E+03	5.0612	4.7619
2.0E+03	5.2050	4.9057
3.0E+03	5.4077	5.1084
4.0E+03	5.5516	5.2523
5.0E+03	5.6631	5.3638
6.0E+03	5.7543	5.4550
8.0E+03	5.8981	5.5988

the long-time approximation applies within 1 percent when

$$t_D > 12.5\left(r_D^2 + \frac{1}{3}\right). \quad \ldots (24)$$

INFINITE-CONDUCTIVITY VERTICAL FRACTURE

The system of linear equations given by Eqs. 17 and 18 must be solved for $2q_m hx_f/q_f$, which represents the ratio of the flux per unit length in the mth segment, q_m, to the flux per unit length in the uniform flux fracture case, $q_f/2hx_f$. The stabilized value of $2q_m hx_f/q_f$ along the half-fracture length is shown in Fig. 5. Although uniform pressure in the fracture can be obtained with as little as 10 segments, it is necessary to use enough divisions to obtain a stabilized value of $\sigma_D(|x_D|<1, 0) = \sigma_{wD}$ in the fracture, as indicated by Fig. 6. The change in σ_{wD} is less than 5×10^{-5} when the number of fracture segments is increased from 59 to 60. In this study, we have used 90 segments to obtain a stabilized value of σ_{wD} in the fracture equal to -0.305. This value of σ_{wD} can be guaranteed to within 0.1 percent. The precision of determination of the dimensionless pressure given by Eq. 14 is, of course, much higher. Eq. 14 then yields for the long-time pressure drop on the fracture,

$$p_{wD}(t_D) = \frac{1}{2}\ln t_D + 1.100. \quad \ldots (25)$$

The same result can be obtained in the uniform flux fracture case by measuring the pressure drop at $x_D = 0.732$ in the fracture. This can be calculated by substituting -0.305 for $\sigma(x_D, 0)$ in Eq. 23. It is obvious in Fig. 7. This suggests that the *pressure drop on the fracture* for the infinite-conductivity fracture can be obtained from that for the *uniform flux fracture*, Eq. 20, with $x_D = 0.732$. The result is

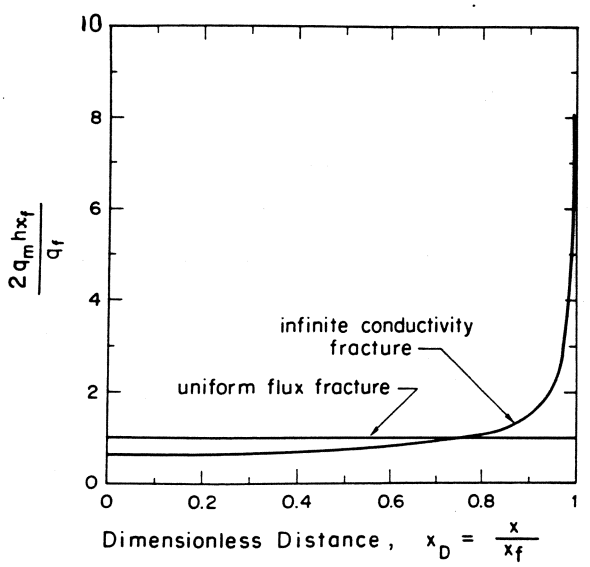

FIG. 5 — STABILIZED FLUX DISTRIBUTION ALONG VERTICAL FRACTURE.

$$p_{wD}(t_D) = \frac{1}{2}\sqrt{\pi t_D}\left[\operatorname{erf}\left(\frac{0.134}{\sqrt{t_D}}\right) + \operatorname{erf}\left(\frac{0.866}{\sqrt{t_D}}\right)\right] - 0.067\ \mathrm{Ei}\left(-\frac{0.018}{t_D}\right) - 0.433\ \mathrm{Ei}\left(-\frac{0.750}{t_D}\right) \quad \ldots\ldots\ldots (26)$$

Eq. 26 yields the correct value of the wellbore pressure for a well with an infinite-conductivity vertical fracture, at early and long times. It can be assumed that it also yields the correct pressure values during the transition period. A similar result ($x_D = 0.75$) has been obtained by Muskat[15] for a well with partial penetration at steady state. $p_{wD}(t_D)$ from Eq. 26 has been listed vs t_D in Table 1, and graphed in Figs. 8 and 9, where it corresponds to the ($x_e/x_f = \infty$) curve.

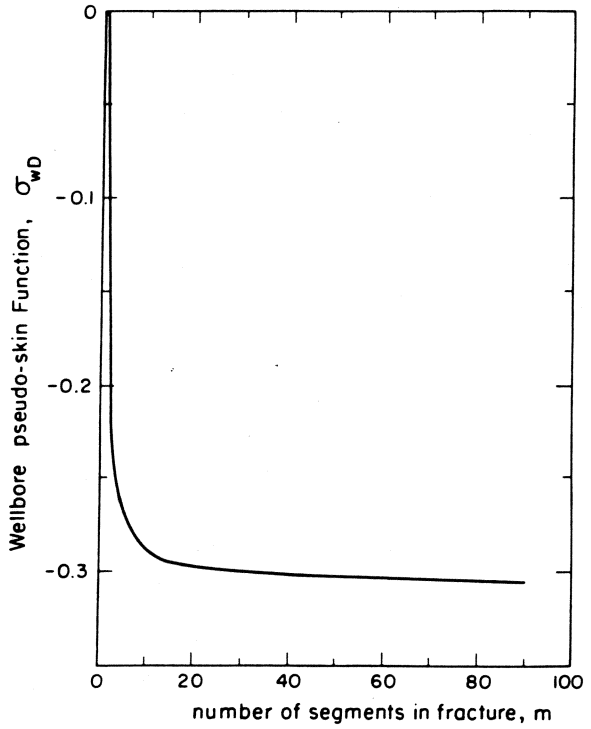

FIG. 6—CONVERGENCE OF THE WELLBORE PSEUDO SKIN FUNCTION σ_{wD} (INFINITE-CONDUCTIVITY FRACTURE).

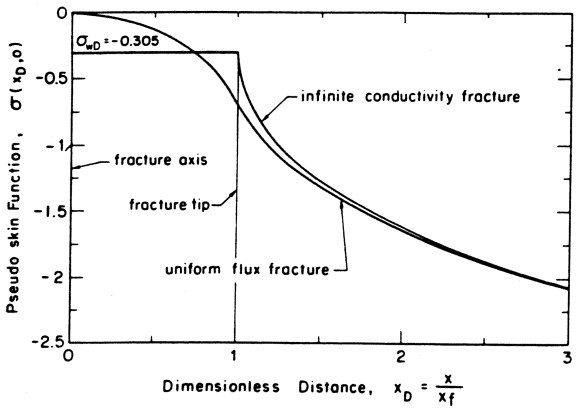

FIG. 7—PSEUDO SKIN FUNCTION VS DIMENSIONLESS DISTANCE.

VERTICALLY FRACTURED WELL IN A RECTANGULAR CLOSED RESERVOIR

When a reservoir is in an early stage of depletion, the production of a particular well is not perturbed by the existence of other wells or by boundary effects. After a while this is no longer true, and a new solution must be developed that considers the reservoir boundaries or the effect of the other wells.

Fig. 10 presents a schematic of a vertically fractured well in a rectangular, closed drainage system. Two types of fracture will be considered — uniform flux and infinite conductivity — but, as in the infinite-reservoir case, it is only necessary to derive the dimensionless pressure drop for the uniform flux fracture. This is obtained immediately

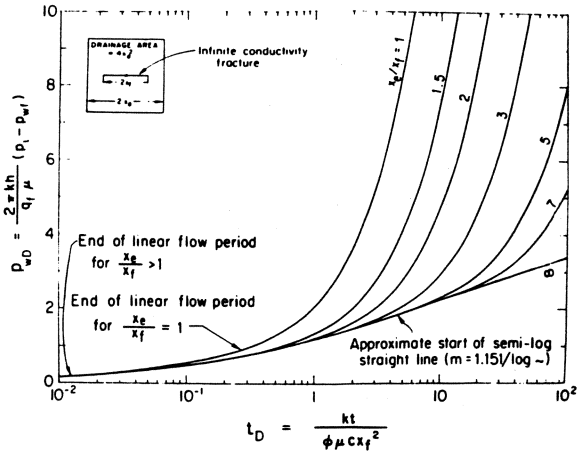

FIG. 8—p_{wD} VS t_D FOR AN INFINITE-CONDUCTIVITY VERTICAL FRACTURE.

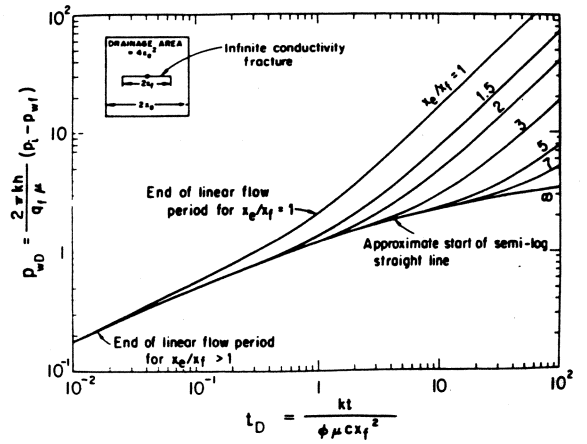

FIG. 9—p_{wD} VS t_D FOR AN INFINITE-CONDUCTIVITY VERTICAL FRACTURE.

by means of the Green's function and product solution method (see Ref. 14). The result is

$$p_D\left(\frac{x}{x_e},\frac{y}{y_e},t_{DA}\right) = 2\pi\int_0^{t_{DA}}\left[1+2\sum_{n=1}^{\infty}\cdot\exp\left(-n^2\pi^2\frac{x_e}{y_e}t'_{DA}\right)\cos n\pi\frac{y_w}{2y_e}\cdot\cos n\pi\frac{y_w+y}{2y_e}\right]\left[1+2\sum_{n=1}^{\infty}\exp\left(-n^2\pi^2\cdot\frac{y_e}{x_e}t'_{DA}\right)\frac{\sin n\pi\frac{x_f}{2x_e}}{n\pi\frac{x_f}{2x_e}}\cos n\pi\frac{x_w}{2x_e}\cdot\cos n\pi\frac{x_w+x}{2x_e}\right]dt'_{DA} \quad \ldots\ldots\ldots (27)$$

where t_{DA} represents the dimensionless time based on the drainage area:

$$t_{DA} = \frac{kt}{\phi\mu c 4(x_e\, y_e)^2} \quad \ldots\ldots (28)$$

The pressure drop on the fracture for a vertical fracture at the center of a square ($x_e = y_e$ and $x_w = y_w$) is then given by

$$p_{wD}(t_{DA}) = 2\pi\int_0^{t_{DA}}\left[1+2\sum_{n=1}^{\infty}\exp(-4n^2\pi^2t'_{DA})\right]\left[1+2\sum_{n=1}^{\infty}\exp(-4n^2\pi^2t'_{DA})\frac{\sin n\pi\frac{x_f}{x_e}}{n\pi\frac{x_f}{x_e}}\cdot\cos n\pi x_D\frac{x_f}{x_e}\right]dt'_{DA} \quad \ldots\ldots (29)$$

The pressure drops on the fracture for a uniform flux fracture and for an infinite-conductivity fracture are obtained by evaluating Eq. 29 at $x_D = 0$ and $x_D = 0.732$, respectively. The choice of the same point as in the infinite case leads to reasonable results and can be justified *a posteriori* by the method of *desuperposition*, presented later in this paper. Numerical values of the dimensionless pressure drop from Eq. 29 are listed vs t_{DA} in Tables 2 and 3, and have been plotted vs t_D (not t_{DA}) in Figs. 3 and 4 and Figs. 8 and 9, respectively, for various values of the x_e/x_f ratio. This ratio is used instead of Russell and Truitt's[8] fracture penetration ratio x_f/x_e because the limiting case of a vertical fracture in a square reservoir is a vertical fracture in an infinite reservoir (Figs. 3, 4, 8, and 9), which correspond to $x_e/x_f = \infty$, whereas a zero fracture penetration ratio ($x_f/x_e = 0$) corresponds to an unfractured well in a square reservoir, which is a different problem.

Three different flow periods can be characterized for both types of fractures: a *linear* flow period occurs at early times. This corresponds to the one-half slope straight line in log-log coordinates (Figs. 4 and 9). After a period of transition, there is a *pseudoradial* flow period corresponding to the semilog straight line (Figs. 3 and 8). After a second period of transition, *pseudosteady* state occurs, which is characterized by an approximate unit slope straight line in log-log coordinates. Depending upon x_e/x_f, one or more of these different flow periods may be missing; in the total fracture penetration case ($x_e/x_f = 1$), for instance, the first transition period and the pseudoradial period do not appear, whereas only the pseudoradial period is missing for values of x_e/x_f between 1 and 3 (uniform flux fracture), or 1 and 5 (infinite-conductivity fracture).

DISCUSSION OF VERTICAL FRACTURE SOLUTIONS

A comparison has been made in Table 4, and in Figs. 11 and 12 between the subject analytical solution for the *infinite-conductivity fracture* and Russell and Truitt's results.[8] As can be seen from Figs. 11 and 12, the smaller the x_e/x_f, the closer the two solutions become at long times. The over-all agreement is good, in view of the fact that the Russell and Truitt solution is an explicit finite-difference solution for a very difficult problem. The total fracture penetration cases ($x_e/x_f = 1$) agree exactly at all times. None of the Russell-Truitt curves, however, produce the 1.1515 slope semilog

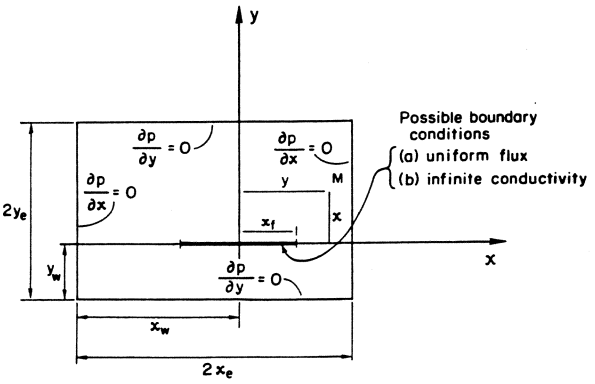

FIG. 10—VERTICAL FRACTURE IN A RECTANGULAR RESERVOIR.

straight line. This result was for many years erroneously thought by one of the authors of this study to be an inherent result of a vertical fracture, rather than an effect caused by the drainage boundaries. Furthermore, at very early times there are some discrepancies in the way the Russell-Truitt curves leave the log-log half-unit slope straight line, which makes them difficult to use with type-curve matching methods. Finally, the difference between the current analytical solution and the Russell-Truitt solution for $x_e/x_f = 10$ is much larger than that for other values of x_e/x_f. This Russell-Truitt case appears to contain an error and is not recommended for further use.

Russell and Truitt did not provide results for a vertically fractured well in an infinite reservoir, but such can be extracted from their results by *desuperposition*. The behavior of a fractured well in a square is identical with that of an infinite system containing a square array of fractured wells. The square array could be constructed by superposition of single fractured wells in infinite

TABLE 2 — p_{wD} FOR A UNIFORM FLUX VERTICAL FRACTURE AT THE CENTER OF A SQUARE

t_{DA} / x_e/x_f	1.00	1.50	2.00	3.00	5.00	7.00	10.00	15.00
1.00E-04	0.0354	0.0532	0.0709	0.1063	0.1772	0.2481	0.3545	0.5306
1.50E-04	0.0434	0.0651	0.0868	0.1302	0.2171	0.3039	0.4340	0.6460
2.00E-04	0.0501	0.0752	0.1003	0.1504	0.2507	0.3509	0.5007	0.7392
3.00E-04	0.0614	0.0921	0.1228	0.1842	0.3070	0.4297	0.6105	0.8855
4.00E-04	0.0709	0.1063	0.1418	0.2127	0.3545	0.4957	0.6999	0.9986
5.00E-04	0.0793	0.1189	0.1585	0.2378	0.3962	0.5533	0.7756	1.0908
6.00E-04	0.0868	0.1302	0.1737	0.2605	0.4340	0.6046	0.8414	1.1686
8.00E-04	0.1003	0.1504	0.2005	0.3008	0.5007	0.6933	0.9515	1.2953
1.00E-03	0.1121	0.1681	0.2242	0.3363	0.5587	0.7686	1.0417	1.3963
1.50E-03	0.1373	0.2059	0.2746	0.4118	0.6790	0.9183	1.2145	1.5846
2.00E-03	0.1585	0.2378	0.3171	0.4752	0.7756	1.0334	1.3427	1.7211
3.00E-03	0.1942	0.2912	0.3883	0.5801	0.9261	1.2057	1.5294	1.9164
4.00E-03	0.2242	0.3363	0.4482	0.6661	1.0417	1.3336	1.6650	200565
5.00E-03	0.2507	0.3760	0.5007	0.7392	1.1355	1.4354	1.7716	2.1658
6.00E-03	0.2746	0.4118	0.5477	0.8030	1.2145	1.5199	1.8594	2.2554
8.00E-03	0.3171	0.4752	0.6297	0.9103	1.3427	1.6554	1.9990	2.3973
1.00E-02	0.3545	0.5306	0.6999	0.9986	1.4447	1.7619	2.1080	2.5078
1.50E-02	0.4342	0.6460	0.8414	1.1686	1.6344	1.9577	2.3073	2.7090
2.00E-02	0.5013	0.7393	0.9515	1.2953	1.7716	2.0981	2.4495	2.8520
3.00E-02	0.6140	0.8861	1.1183	1.4804	1.9676	2.2974	2.6505	3.0541
4.00E-02	0.7092	1.0011	1.2443	1.6159	2.1086	2.4400	2.7940	3.1980
5.00E-02	0.7935	1.0973	1.3470	1.7241	2.2201	2.5524	2.9069	3.3111
6.00E-02	0.8708	1.1819	1.4356	1.8161	2.3140	2.6469	3.0016	3.4061
8.00E-02	1.0127	1.3315	1.5893	1.9734	2.4732	2.8067	3.1618	3.5664
1.00E-01	1.1458	1.4678	1.7273	2.1129	2.6136	2.9473	3.3025	3.7072
1.50E-01	1.4652	1.7895	2.0502	2.4368	2.9381	3.2720	3.6273	4.0320
2.00E-01	1.7801	2.1047	2.3655	2.7523	3.2537	3.5876	3.9429	4.4477
3.00E-01	2.4086	2.7332	2.9941	3.3808	3.8823	4.2162	4.5715	4.9762
4.00E-01	3.0369	3.3615	3.6224	4.0092	4.5106	4.8445	5.1998	5.6045
5.00E-01	3.6652	3.9898	4.2507	4.6375	5.1389	5.4728	5.8281	6.2328
6.00E-01	4.2935	4.6181	4.8790	5.2658	5.7672	6.1011	6.4564	6.8512
8.00E-01	5.5501	5.8748	6.1357	6.5224	7.0239	7.3578	7.7131	8.1178
1.00E+00	6.8068	7.1314	7.3923	7.7791	8.2805	8.6144	8.9697	9.3744
1.50E+00	9.9484	10.2730	10.5339	10.9207	11.4221	11.7560	12.1113	12.5160
2.00E+00	13.0900	13.4146	13.6755	14.0623	14.5637	14.8976	15.2529	15.6576
3.00E+00	19.3732	19.6978	19.9587	20.3455	20.8469	21.1808	21.5361	21.9408
4.00E+00	25.6563	25.9810	26.2418	26.6286	27.1301	27.4639	27.8193	28.2240
5.00E+00	31.9395	32.3641	32.5250	32.9118	33.4132	33.7471	34.1024	34.5072
6.00E+00	38.2227	38.5473	38.8082	39.1950	39.6964	40.0303	40.3856	40.7904
8.00E+00	50.7891	51.1137	51.3746	51.7614	52.2628	52.5967	52.9520	53.3567

mediums in the same way a well in a closed square was constructed by Matthews *et al.*[18] and by Earlougher *et al.*[19] We realize that the pressure drop at a great distance from a fractured well produced at constant rate is essentially identical with the pressure drop caused by an unfractured well. Thus, the behavior of a fractured well in a closed square may be approximated by generating the drainage boundaries with unfractured wells, if x_e/x_f is large enough. This simple approach can also be used to extract the behavior of a fractured well in an infinite medium from that of a fractured well in a closed square. This can be stated as follows: the p_D for a fractured well in an infinite medium is equal to the p_D for a fractured well in a closed square, less the p_D for an unfractured well in a closed square, plus the p_D for an unfractured well in an infinite medium. The method has been applied to both the current analytical solutions and Russell-Truitt solutions for an infinite-conductivity fracture in a closed square reservoir (Table 4 and Fig. 13). The data for an unfractured well in a

TABLE 3 — p_{wD} FOR AN INFINITE-CONDUCTIVITY VERTICAL FRACTURE AT THE CENTER OF A SQUARE

t_{DA} / x_e/x_f	1.00	1.50	2.00	3.00	5.00	7.00	10.00	15.00
1.00E-04	0.0354	0.0532	0.0709	0.1063	0.1765	0.2433	0.3356	0.4735
1.50E-04	0.0434	0.0651	0.0868	0.1302	0.2145	0.2928	0.3996	0.5590
2.00E-04	0.0501	0.0752	0.1003	0.1502	0.2456	0.3327	0.4509	0.6278
3.00E-04	0.0614	0.0921	0.1228	0.1832	0.2955	0.3962	0.5328	0.7379
4.00E-04	0.0709	0.1063	0.1417	0.2104	0.3356	0.4471	0.5987	0.8259
5.00E-04	0.0793	0.1139	0.1582	0.2338	0.3697	0.4904	0.6549	0.9000
6.00E-04	0.0868	0.1302	0.1730	0.2545	0.3996	0.5284	0.7042	0.9642
8.00E-04	0.1003	0.1502	0.1989	0.2901	0.4509	0.5939	0.7889	1.0718
1.00E-03	0.1121	0.1676	0.2212	0.3204	0.4945	0.6496	0.8603	1.1600
1.50E-03	0.1373	0.2040	0.2671	0.3821	0.5833	0.7631	1.0027	1.3296
2.00E-03	0.1585	0.2338	0.3041	0.4315	0.6549	0.8536	1.1129	1.4560
3.00E-03	0.1942	0.2818	0.3633	0.5104	0.7691	0.9953	1.2792	1.6405
4.00E-03	0.2242	0.3204	0.4107	0.5738	0.8603	1.1050	1.4037	1.7750
5.00E-03	0.2507	0.3533	0.4509	0.6278	0.9367	1.1947	1.5033	1.8808
6.00E-03	0.2746	0.3821	0.4863	0.6753	1.0027	1.2707	1.5862	1.9681
8.00E-03	0.3171	0.4315	0.5470	0.7569	1.1129	1.3948	1.7196	2.1071
1.00E-02	0.3545	0.4735	0.5987	0.8259	1.2030	1.4941	1.8248	2.2158
1.50E-02	0.4342	0.5595	0.7043	0.9642	1.3754	1.6800	2.0189	2.4146
2.00E-02	0.5013	0.6295	0.7891	1.0718	1.5033	1.8152	2.1583	2.5564
3.00E-02	0.6140	0.7445	0.9239	1.2352	1.6896	2.0092	2.3567	2.7572
4.00E-02	0.7092	0.8406	1.0316	1.3592	1.8256	2.1492	2.4989	2.9006
5.00E-02	0.7935	0.9254	1.1235	1.4607	1.9342	2.2600	2.6110	3.0133
6.00E-02	0.8708	1.0030	1.2054	1.5486	2.0264	2.3536	2.7053	3.1081
8.00E-02	1.0127	1.1452	1.3521	1.7015	2.1838	2.5124	2.8649	3.2682
1.00E-01	1.1458	1.2784	1.4872	1.8392	2.3234	2.6527	3.0055	3.4089
1.50E-01	1.4652	1.5979	1.8081	2.1619	2.6474	2.9771	3.3301	3.7337
2.00E-01	1.7801	1.9128	2.1231	2.4772	2.9629	3.2926	3.6457	4.0493
3.00E-01	2.4086	2.5413	2.7516	3.1057	3.5915	3.9212	4.2743	4.6778
4.00E-01	3.0369	3.1696	3.3799	3.7341	4.2198	4.5495	4.9026	5.3061
5.00E-01	3.6652	3.7979	4.0082	4.3624	4.8481	5.1778	5.5309	5.9345
6.00E-01	4.2935	4.4262	4.6366	4.9907	5.4764	5.8061	6.1592	6.5628
8.00E-01	5.5501	5.6829	5.8932	6.2473	6.7331	7.0628	7.4159	7.8194
1.00E+00	6.8068	6.9395	7.1498	7.5040	7.9897	8.3194	8.6725	9.0761
1.50E+00	9.9484	10.0811	10.2914	10.6456	11.1313	11.4610	11.8141	12.2177
2.00E+00	13.0900	13.2227	13.4330	13.7872	14.2729	14.6026	14.9557	15.3592
3.00E+00	19.3732	19.5059	19.7162	20.0703	20.5561	20.8858	21.2389	21.6424
4.00E+00	25.6563	25.7891	25.9994	26.3535	26.8393	27.1690	27.5220	27.9256
5.00E+00	31.9395	32.0722	32.2826	32.6367	33.1224	33.4521	33.8052	34.2088
6.00E+00	38.2227	38.3554	38.5658	38.9199	39.4056	39.7353	40.0884	40.4920
8.00E+00	50.7891	50.9218	51.1321	51.4863	51.9720	52.3017	52.6548	53.0584

closed square were taken from Table 1, Ref. 19. It was found that desuperposition of the analytical solution for a closed square yields a very good approximation of the analytical solution for an infinite reservoir, for x_e/x_f values of 2, 5, and 10/3. This justifies *a posteriori* the choice of x_D = 0.732 for representing the wellbore pressure for an infinite-conductivity fracture in the finite-reservoir case. x_e/x_f ratios of 10/7 and 1 gives p_D values that are much too large, implying that desuperposition cannot be used because the fracture is too close to the square boundary. The x_e/x_f = 10 case yields p_D values by desuperposition that are far too small. It is likely that the Russell and Truitt results have a small, almost constant error for this case. It should be noted, however, that the Russell and Truitt desuperposed solution for an infinite reservoir does have a slope of 1.151 when plotted on semilog coordinates, although their solutions for the closed square did not.

An interesting interpretation of the behavior of a vertically fractured well can be made in terms of an equivalent unfractured system. Prats[5] has shown that an infinite-conductivity vertical fracture, producing an incompressible fluid from a closed circular reservoir *at steady state*, is equivalent to an unfractured well with an effective radius equal to a quarter of the total fracture length, for ratios of the reservoir radius to the fracture half length greater than 2. The same is true, within 7 percent,

TABLE 4 — COMPARISON BETWEEN ANALYTICAL AND FINITE-DIFFERENCE WELLBORE PRESSURES FOR AN INFINITE-CONDUCTIVITY VERTICAL FRACTURE AT THE CENTER OF A CLOSED SQUARE

t_{DA} / x_e/x_f=1	1		10/7		2	
	Analytical	Finite Dif.	Analytical	Finite Dif.	Analytical	Finite Dif.
1.0 E-04	0.0354	0.0355	0.0506	0.0506	0.0709	0.0709
2.0 E-04	0.0501	0.0501	0.0716	0.0716	0.1003	0.1003
5.0 E-04	0.0793	0.0793	0.1132	0.1107	0.1582	0.1527
8.0 E-04	0.1003		0.1431		0.1989	
1.0 E-03	0.1121	0.1121	0.1598	0.1528	0.2212	0.2092
2.0 E-03	0.1585	0.1585	0.2233	0.2111	0.3041	0.2870
5.0 E-03	0.2507	0.2507	0.3386	0.3220	0.4509	0.4326
8.0 E-03	0.3171	0.3171	0.4142	0.3982	0.5470	0.5306
1.0 E-02	0.3545	0.3545	0.4548	0.4398	0.5987	0.5836
2.0 E-02	0.5013	0.5014	0.6062	0.5969	0.7891	0.7755
5.0 E-02	0.7935	0.7936	0.8973	0.8947	1.1235	1.1051
8.0 E-02	1.0127	1.0127	1.1160	1.1145	1.3521	1.3309
1.0 E-01	1.1458	1.1457	1.2489	1.2477	1.4872	1.4654
2.0 E-01	1.7801	1.7797	1.8832	1.8818	2.1231	2.1003
5.0 E-01	3.6652	3.6648	3.7683	3.7668	4.0082	3.9853
8.0 E-01	5.5501	5.5498	5.6532	5.6517	5.8932	5.8702
1.0 E+00	6.8068	6.8064	6.9099	6.9034	7.1498	7.1269
2.0 E+00	13.0900	13.0696	13.1930	13.1916	13.4330	13.4101
5.0 E+00	31.9395		32.0426		32.2826	
8.0 E+00	50.7891		50.8922		51.1321	

t_{DA} / x_e/x_f=1	10/3		5		10	
	Analytical	Finite Dif.	Analytical	Finite Dif.	Analytical	Finite Dif.
1.0 E-04	0.1181	0.1182	0.1765	0.1772	0.3356	0.3545
2.0 E-04	0.1666	0.1671	0.2456	0.2476	0.4509	0.4715
5.0 E-04	0.2578	0.2463	0.3697	0.3575	0.6549	0.6395
8.0 E-04	0.3187		0.4509		0.7889	
1.0 E-03	0.3514	0.3318	0.4945	0.4780	0.8603	0.8013
2.0 E-03	0.4711	0.4480	0.6549	0.6390	1.1129	1.0171
5.0 E-03	0.6830	0.6586	0.9367	0.9164	1.5033	1.3697
8.0 E-03	0.8220	0.7951	1.1129	1.0872	1.7196	1.5732
1.0 E-02	0.8958	0.8668	1.2030	1.1742	1.8248	1.6735
2.0 E-02	1.1550	1.1167	1.5033	1.4659	2.1583	1.9970
5.0 E-02	1.5552	1.5045	1.9342	1.8894	2.6110	2.4430
8.0 E-02	1.7984	1.7442	2.1838	2.1372	2.8649	2.6958
1.0 E-01	1.9366	1.8817	2.3234	2.2766	3.0055	2.8361
2.0 E-01	2.5751	2.5189	2.9629	2.9154	3.6457	3.4757
5.0 E-01	4.4602	4.4039	4.8481	4.8004	5.5309	5.3607
8.0 E-01	6.3452	6.2889	6.7331	6.6853	7.4159	7.2456
1.0 E+00	7.6018	7.5455	7.9897	7.9419	8.6725	8.5023
2.0 E+00	13.8850	13.8287	14.2729	14.2252	14.9557	14.7855
5.0 E+00	32.7345		33.1224		33.8052	
8.0 E+00	51.5841		51.9720		52.6548	

for a compressible fluid at *steady* or *pseudosteady* state.[6] We can see that these results apply to a vertically fractured well in an infinite reservoir during the *pseudoradial* period, because Eq. 25 can be written as

$$p_{wD}(t_D) = \frac{1}{2}\left[\ln\left(\frac{kt}{\phi\mu c\left(\frac{x_f}{2}\right)^2}\right) + 0.80907\right] \quad \ldots\ldots\ldots \quad (30)$$

The effective well radius for an infinite-conductivity vertical fracture in an infinite reservoir is thus exactly one-fourth the total fracture length. The effective radius for an infinite-conductivity vertical fracture in a closed square reservoir at *pseudosteady state* may be obtained from the general pseudosteady-state depletion equation presented by Brons and Miller,[20] which, in the present case, can be expressed as

$$p_{wD} = 2\pi\, t_{DA} + \ln \frac{4(x_f/r'_w)}{\sqrt{e^{\gamma} C_A}} \frac{x_e}{x_f}, \quad \ldots \quad (31)$$

where C_A is the shape factor for a well in a square, and r'_w is the effective well radius. Effective radii computed from the current analytical solution and from the Russell and Truitt solution are compared in Fig. 14 with the results of Prats *et al.*[6] for various values of x_f/x_e (x_f/x_e is used for convenience in this case). Surprisingly, variations of the radii as a function of x_f/x_e are different in the Prats *et al.* results. Again, the result for x_f/x_e = 0.1 in Russell-Truitt's case is inconsistent with other results.

Comparison was also made between the subject solution and the analytical results of van Everdingen and Meyer[11] for an infinite-conductivity fracture in an infinite reservoir. Although not shown, results do not compare well. The van Everdingen and Meyer solution is correct during the initial linear flow period. But it yields a semilog straight line of slope 0.576 per $\log_{10}$ cycle, instead of 1.151 per $\log_{10}$ cycle as in the subject study, or as in the Russell and Truitt[8] desuperposed solution. It is not recommended that this solution be used in the pseudoradial flow period. Either the current analytical solution, or the desuperposed Russell-Truitt solution for a fractured well in an infinite medium may be used.

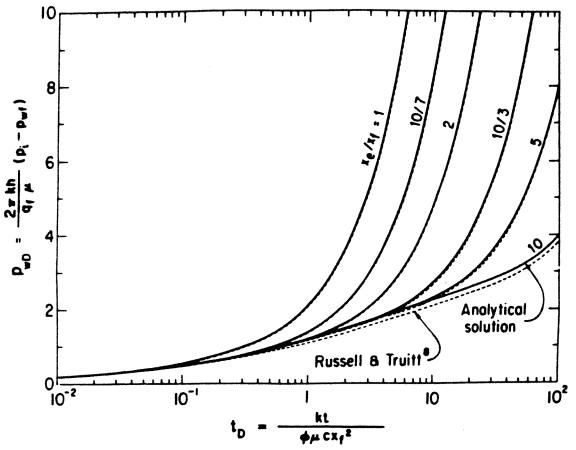

FIG. 11 — COMPARISON OF ANALYTICAL SOLUTION AND RUSSELL AND TRUITT SOLUTION FOR AN INFINITE-CONDUCTIVITY VERTICAL FRACTURE IN A SQUARE.

NOMENCLATURE

C_A = pseudosteady-state shape factor for a well at the center of a square[19] = 30.86

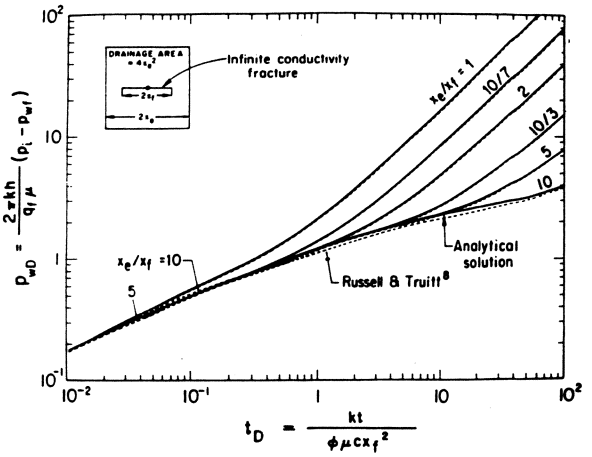

FIG. 12 — COMPARISON OF ANALYTICAL SOLUTION AND RUSSELL AND TRUITT SOLUTION FOR AN INFINITE-CONDUCTIVITY VERTICAL FRACTURE IN A CLOSED SQUARE.

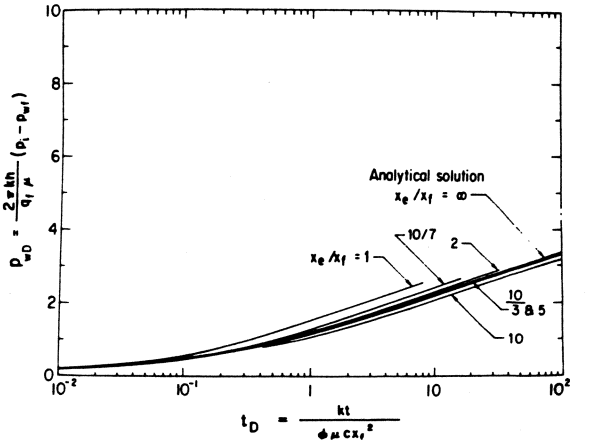

FIG. 13 — DESUPERPOSITION OF RUSSELL AND TRUITT RESULTS TO OBTAIN A VERTICALLY FRACTURED WELL IN AN INFINITE RESERVOIR AND COMPARISON WITH THE SUBJECT ANALYTICAL SOLUTION FOR AN INFINITE-CONDUCTIVITY VERTICAL FRACTURE IN AN INFINITE RESERVOIR.

h = formation thickness
k = formation permeability
M = number of vertical fracture elements for generating an infinite-conductivity fracture
p = pressure
p_i = initial reservoir pressure
p_D = dimensionless pressure
q_f = total withdrawal rate from fracture
q_m = flux per unit area in vertical fracture elements
r = distance to fracture axis
r_D = dimensionless distance to fracture axis, based on fracture half length
r'_w = effective well radius
t = flowing time
t_D = dimensionless time based on the fracture half length
t'_D = dummy variable of integration
t_{DA} = dimensionless time based on drainage area
x,y = space coordinates
x_D, y_D = dimensionless coordinates based on the fracture half length
x_e, y_e = rectangular reservoir half dimensions
x_f = fracture half length
x_w, y_w = fracture axis coordinates
γ = Euler's constant = 0.5772
η = diffusivity constant
μ = fluid viscosity

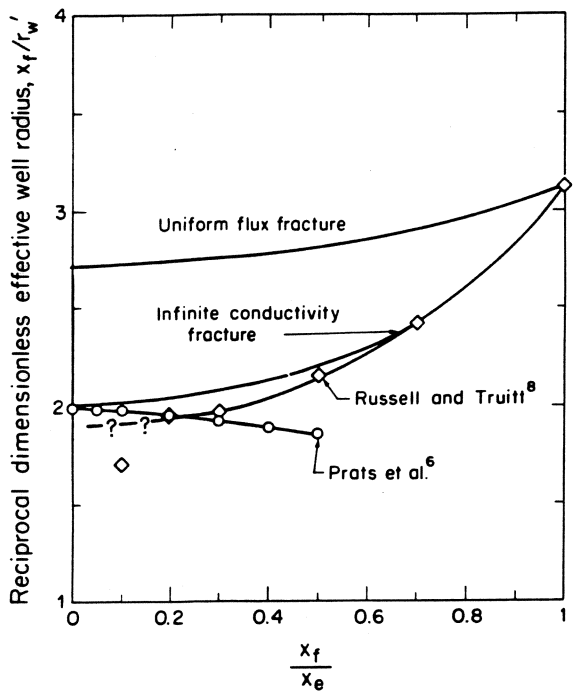

FIG. 14—COMPARISON OF RECIPROCAL DIMENSIONLESS EFFECTIVE WELL RADIUS, x_f/r'_w.

σ = pseudo skin function, defined by Eq. 14
τ = dummy variable of integration
ϕ = formation porosity

SPECIAL FUNCTIONS

Inverse tangent function:

$$\arctan(x) = \tan^{-1}(x)$$

Exponential integral:

$$-Ei(-x) = \int_0^x \frac{e^{-u}}{u}\,du$$

Error function:

$$erf(x) = \frac{2}{\sqrt{\pi}} \int_0^x e^{-u^2}\,du$$

Complementary error function:

$$erfc(x) = 1 - erf(x)$$

Units: CGS units are used throughout this study.

ACKNOWLEDGMENTS

We acknowledge the financial assistance of the Miller Institute for Basic Research in Science, U. of California at Berkeley. We are also thankful to Texaco and the Mobil Foundation for financial aid. Computer time was contributed by the Computer Center of the U. of California and by Stanford U.

In addition, helpful correspondence has been conducted with a number of persons. Conversations with A. F. van Everdingen and L. Joffre Meyer formed part of the inspiration for this study. We are deeply grateful to R. A. Morse and W. D. von Gonten of Texas A&M U. for finite-difference-solution results, which aided in establishing correct vertical-fracture solutions. Finally, helpful comments were also received from D. G. Russell of Shell Development Co.

REFERENCES

1. Ramey, H. J., Jr.: "Short-Time Well Test Data Interpretation in the Presence of Skin Effect and Wellbore Storage," *J. Pet. Tech.* (Jan. 1970) 97-104; *Trans.*, AIME, Vol. 249.
2. Agarwal, R., Al-Hussainy, R., and Ramey, H. J., Jr.: "An Investigation of Wellbore Storage and Skin Effect in Unsteady Liquid Flow: I — Analytical Treatment," *Soc. Pet. Eng. J.* (Sept. 1970) 279-290; *Trans.*, AIME, Vol. 249.
3. Dyes, A. B., Kemp, C. E., and Caudle, B. H.: "Effect of Fractures on Sweep-Out Pattern," *Trans.*, AIME (1958) Vol. 213, 245-249.
4. McGuire, W. J., and Sikora, V. J.: "The Effect of Vertical Fractures on Well Productivity," *Trans.*, AIME (1960) Vol. 219, 401-403.
5. Prats, M.: "Effect of Vertical Fractures on Reservoir Behavior — Incompressible Fluid Case," *Soc. Pet. Eng. J.* (June 1961) 105-118; *Trans.*, AIME, Vol. 222.

6. Prats, M., Hazebroek, P., and Strickler, W. R.: "Effect of Vertical Fractures on Reservoir Behavior — Compressible-Fluid Case," *Soc. Pet. Eng. J.* (June 1962) 87-94; *Trans.*, AIME, Vol. 225.

7. Scott, J. P.: "The Effect of Vertical Fractures on Transient Pressure Behavior of Wells," *J. Pet. Tech.* (Dec. 1963) 1365-1370; *Trans.*, AIME, Vol. 228.

8. Russell, D. G., and Truitt, N. E.: "Transient Pressure Behavior in Vertically Fractured Reservoirs," *J. Pet. Tech.* (Oct. 1964) 1159-1170; *Trans.*, AIME, Vol. 231.

9. Millheim, K., and Cichowicz, L.: "Testing and Analyzing Low-Permeability Fractured Gas Wells," *J. Pet. Tech.* (Feb. 1968) 193-198; *Trans.*, AIME, Vol. 243.

10. Wattenbarger, R. A., and Ramey, H. J., Jr.: "Well Test Interpretation of Vertically Fractured Gas-Wells," *J. Pet. Tech.* (May 1969) 625-632; *Trans.*, AIME, Vol. 246.

11. van Everdingen, A. F., and Meyer, L. J.: "Analysis of Buildup Curves Obtained After Well Treatment," *J. Pet. Tech.* (April 1971) 513-524; *Trans.*, AIME, Vol. 251.

12. Gringarten, A. C.: "Unsteady-State Pressure Distributions Created by a Well with a Single Horizontal Fracture, Partial Penetration, or Restricted Entry," PhD dissertation, Stanford U. (1971) (Order #71-23, 512 University Microfilms, P.O. Box 1764, Ann Arbor, Mich. 48106).

13. Gringarten, A. C., and Ramey, H. J., Jr.: "Unsteady-State Pressure Distributions Created by a Well with a Single Horizontal Fracture, Partial Penetration, or Restricted Entry," *Soc. Pet. Eng. J.* (Aug. 1974) 413-426; *Trans.*, AIME, Vol. 257.

14. Gringarten, A. C., and Ramey, H. J., Jr.: "The Use of the Point Source Solution and Green's Functions for Solving Unsteady Flow Problems in Reservoirs," *Soc. Pet. Eng. J.* (Oct. 1973) 285-296; *Trans.*, AIME, Vol. 255.

15. Muskat, M.: *The Flow of Homogeneous Fluids Through Porous Media*, J. W. Edwards, Inc., Ann Arbor, Mich. (1946) 273.

16. Burns, W. A., Jr.: Discussion on "Effect of Anisotropy and Stratification on Pressure Transient Analysis of Wells with Restricted Flow Entry," *J. Pet. Tech.* (May 1969) 646-647.

17. Matthews, C. S., and Russell, D. G.: *Pressure Build-Up and Flow Tests in Wells*, Monograph Series, Society of Petroleum Engineers of AIME, Dallas (1967) Vol. 1, 11.

18. Matthews, C. S., Brons, F., and Hazebroek, R.: "A Method for Determination of Average Pressure in a Bounded Reservoir," *Trans.*, AIME (1954) Vol. 201, 182-191.

19. Earlougher, R. C., Jr., Ramey, H. J., Jr., Miller, F. G., and Mueller, T. D.: "Pressure Distributions in Rectangular Reservoirs," *J. Pet. Tech.* (Feb. 1968) 199-208; *Trans.*, AIME, Vol. 243.

20. Brons, F., and Miller, W. C.: "A Simple Method for Correcting Spot Pressure Readings," *J. Pet. Tech.* (Aug. 1961) 803-805; *Trans.*, AIME, Vol. 222.

21. Bilhartz, H. L., Jr.: "Effects of Wellbore Damage and Storage on Behavior of Partially-Penetrating Wells," PhD dissertation, Stanford U., Stanford, Calif. (1973).

22. Carslaw, H. S., and Jaeger, J. C.: *Conduction of Heat in Solids*, 2nd ed., Oxford at the Clarendon Press (1959).

23. Carter, R. D., and Tracy, G. W.: "An Improved Method for Calculating Water Influx," *Trans.*, AIME (1960) Vol. 219, 415-417.

***